

Shapes for maximal coverage for two-dimensional random sequential adsorption

Michał Cieśla* and Grzegorz Pająk†

*M. Smoluchowski Institute of Physics, Department of Statistical Physics,
Jagiellonian University, Łojasiewicza 11, 30-348 Kraków, Poland.*

Robert M. Ziff‡

*Center for the Study of Complex Systems and Department of Chemical Engineering,
University of Michigan, Ann Arbor MI 48109-2136 USA.*

(Dated: June 12, 2019)

The random sequential adsorption of various particle shapes is studied in order to determine the influence of particle anisotropy on the saturated random packing. For all tested particles there is an optimal level of anisotropy which maximizes the saturated packing fraction. It is found that a concave shape derived from a dimer of disks gives a packing fraction of 0.5833, which is comparable to the maximum packing fraction of ellipsoids and spherocylinders and higher than any other studied shape. Discussion why this shape is so beneficial for random sequential adsorption is given.

PACS numbers: 05.45.Df, 68.43.Fg

I. INTRODUCTION

Random sequential adsorption (RSA) is a fundamental problem that has attracted unabated interest for decades. In 1939, Flory [1] studied the attachment of blocking pendant groups on a linear polymer, which is effectively a one-dimensional RSA problem. Rényi [2] introduced another famous one-dimensional RSA problem—the parking of cars along an unmarked curb. Feder [3] helped to make RSA a very popular tool for modeling monolayers obtained as a result of irreversible adsorption [4–6]. More recently, random packings generated by RSA have been of interest in a number of scientific fields, e.g., soft matter [7–9], mathematics [10], telecommunication [11] and information theory [12].

The RSA algorithm is based on consecutive tries to add a particle to a packing. Firstly, a particle’s position (and orientation in case of anisotropic objects) is drawn according to the probability distribution which reflects the structure of an underlying surface – a homogeneous surface corresponds to the uniform probability distribution. Then the particle is tested if it overlaps or intersects with any of particles already added to the packing. If not, the particle is added to the packing; otherwise it is abandoned. These steps should be continued until the packing is saturated, i.e., there is no room for any additional particle on a surface. However, typically an algorithm is stopped when the probability of successful adding of a particle is sufficiently small, and extrapolations are made to estimate the maximum “jamming” coverage.

The properties of packings generated by RSA algorithm have been checked for a number of different particle shapes, e.g., spheres [3, 13, 14], spherocylinders

and ellipsoids [15, 16], rectangles [17, 18], and polymers [19, 20]. Results obtained for anisotropic particles show that saturated random coverage fraction reaches its maximum for moderate anisotropy, i.e., when long to short particle axis ratio is approximately 1.5-2.0 [15, 18]. The highest saturated coverage fraction obtained was $\theta_{\max} = 0.583 \pm 0.001$, for both ellipsoids and spherocylinders [15, 16]. Both of these are convex shapes. The highest saturated coverage fraction for concave particles was observed for a dimer built of two overlapping disks, with $\theta_{\max} = 0.5793 \pm 0.0001$ [21], slightly lower than above values.

The primary aim of this study is to analyze set of different concave shapes in order to find if one of them can give a higher saturated random packing fraction than previously found. This will help in designing particles, such as nanoparticles, that can cover a surface most efficiently. Additionally, we want to study the kinetics of RSA for nearly symmetric particles as they appear to be very sensitive on particle shape anisotropy [21, 22].

II. MODEL

The shapes we consider are shown in Fig. 1. Dimers, trimers, tetramers and hexamers are built of identical disks of unit radius, and the distance between neighboring disks centers is $2x$. Parameter x if not stated otherwise was taken from the interval $[0, 1]$. For $x = 0$ all these shapes are equal to a single disk, which of course is isotropic, while for $x = 1$ each disk touches two neighboring disks as presented in the upper row of Fig. 1. Note that the space inside ring of disks also belongs to the particle. Such choice of shapes originates from [21], where properties of dimer random packings were carefully studied. Here we want to test how the more complex shape of particle shape affects properties of saturated random packing. The last shape is built of two partially overlapping squares of a unit side size. Parameter a shown

* michal.ciesla@uj.edu.pl

† grzegorz@th.if.uj.edu.pl

‡ rziff@umich.edu

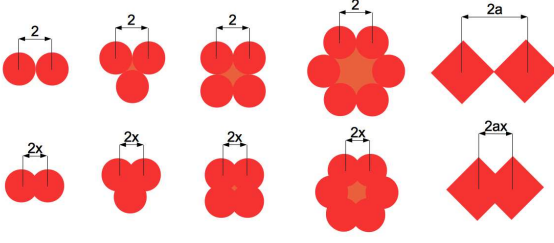


Figure 1. The five types of shapes for which saturated random packings are studied. Disks have a unit radius, and parameter $x \in [0, 1]$ corresponds to half the distance between closest spheres or squares. Squares have a unit side size, thus parameter a equals $\sqrt{2}/2$.

in Fig. 1 equals to $\sqrt{2}/2$. This shape is an analogue of generalized dimer but instead of disks, it is built of two squares. The surface area, for $0 \leq x \leq 1$, of dimer (S_2), trimer (S_3), tetramer (S_4), hexamer (S_6) and the square dimer (S_{2S}) presented in Fig. 1 are given respectively:

$$S_2(x) = 2\pi - 2 \left(\arccos x - x\sqrt{1-x^2} \right) \quad (1)$$

$$\begin{aligned} S_3(x) = & \pi(3 \mp 1)/2 + \arcsin x + \sqrt{3}x^2 + 4x\sqrt{1-x^2} \\ & + \arcsin \left(\frac{1}{2} (x - \sqrt{3-3x^2}) \right) \\ & \pm \arcsin \left(\frac{1}{2} (x + \sqrt{3-3x^2}) \right) \\ & \pm \frac{1}{4} x \sqrt{2x^2 - 2x\sqrt{3-3x^2} + 1} \\ & + \frac{1}{4} x \sqrt{2x^2 + 2x\sqrt{3-3x^2} + 1} \\ & \pm \frac{\sqrt{3}}{4} \sqrt{(x^2-1)(-2x^2+2x\sqrt{3-3x^2}-1)} \\ & - \frac{\sqrt{3}}{4} \sqrt{(x^2-1)(-2x^2-2x\sqrt{3-3x^2}-1)} \quad (2) \end{aligned}$$

$$S_4(x) = \pi + 4x^2 + 4x\sqrt{1-x^2} + 4 \arcsin x \quad (3)$$

$$\begin{aligned} S_6(x) = & \pi(3 \mp 3)/2 + 2 \arcsin x + 6\sqrt{3}x^2 + 8x\sqrt{1-x^2} \\ & + (1 \pm 1) \left[\arcsin(\sqrt{3}x) + \arcsin(\sqrt{1-3x^2}) \right] \\ & + 2 \arcsin \left(\frac{1}{2} (x - \sqrt{3-3x^2}) \right) \\ & \pm 2 \arcsin \left(\frac{1}{2} (x + \sqrt{3-3x^2}) \right) \\ & \pm \frac{1}{2} x \sqrt{2x^2 - 2x\sqrt{3-3x^2} + 1} \\ & + \frac{1}{2} x \sqrt{2x^2 + 2x\sqrt{3-3x^2} + 1} \\ & \pm \frac{\sqrt{3}}{2} \sqrt{(x^2-1)(-2x^2+2x\sqrt{3-3x^2}-1)} \\ & - \frac{\sqrt{3}}{2} \sqrt{(x^2-1)(-2x^2-2x\sqrt{3-3x^2}-1)} \quad (4) \end{aligned}$$

$$S_{2S}(x) = 2(1 + 2x - x^2), \quad (5)$$

where in $S_3(x)$ and $S_6(x)$, the upper sign in \pm or \mp is for $0 \leq x < 1/2$, and the lower sign is for $1/2 \leq x \leq 1$.

These shapes were thrown onto a square surface of a side size up to 1000 with an area up to $S_C = 10^6$. We decided to use open boundary conditions similar to [21]. Such a choice allowed us to use data published there for comparison purposes. The packing fraction is equal to:

$$\theta(t) = N(t) \frac{S_p}{S_C} = \rho(t) S_p, \quad (6)$$

where S_p is a particle surface area and $N(t)$ is a number of particles in a packing after a number of RSA iterations corresponding to time t measured in the dimensionless time units

$$t = n \frac{S_p}{S_C}, \quad (7)$$

where n is number of RSA algorithm steps, and $\rho(t) = N(t)/S_C$ is the surface density of particles in a packing.

The simulation was stopped when $t = 10^5$. At this moment, the probability that a randomly chosen place is large enough for an additional particle is well below 10^{-6} . The number of particles in a single random packing was at the order of 10^5 . To improve statistics, up to 100 independent simulations were performed for each shape. During the simulations the number of particles in a packing $N(t)$ was recorded.

III. RESULTS

Fragments of sample packings are presented in Fig. 2. Examples of dimer packings have been shown in [21]. The

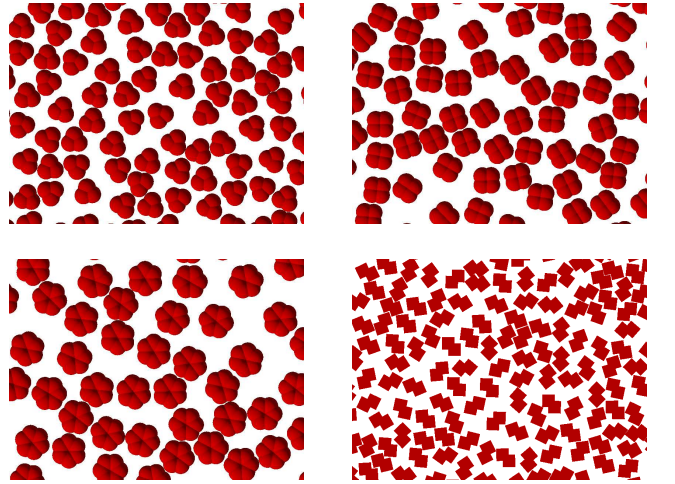


Figure 2. Examples of obtained random packings for studied shapes after $t = 10^5$ iterations of RSA algorithm. Parameter x equals 0.5 for all four shapes.

total number of RSA algorithm steps is large, but finite.

Thus, the resulting packings may be not be saturated. To find number of particles in saturated packing from a finite-time simulation a knowledge about RSA kinetics is essential. Therefore, to study saturated packing fractions the kinetics of the process has to be clarified first.

A. RSA kinetics

The RSA kinetics for large enough time t is governed by the power law [23, 24]

$$\theta(t) = \theta_{\max} - At^{-1/d} \quad (8)$$

where $\theta_{\max} \equiv \theta(t \rightarrow \infty)$, A is a positive constant and d depends on particle shape and properties of a surface. For flat and homogeneous surfaces d can be interpreted as a number of degrees of freedom of a particle [19, 25]. Thus, for RSA of disks on two dimensional flat surface $d = 2$ but for anisotropic particles $d = 3$ as an orientation of a particle is an additional degree of freedom. It is worth noting, that even when particle anisotropy is very small, $d = 3$ describes the ultimate asymptotic behavior [15, 21, 22].

The RSA kinetics of our shapes are presented in Fig. 3. Data for dimers has been presented in [21]. For all shapes

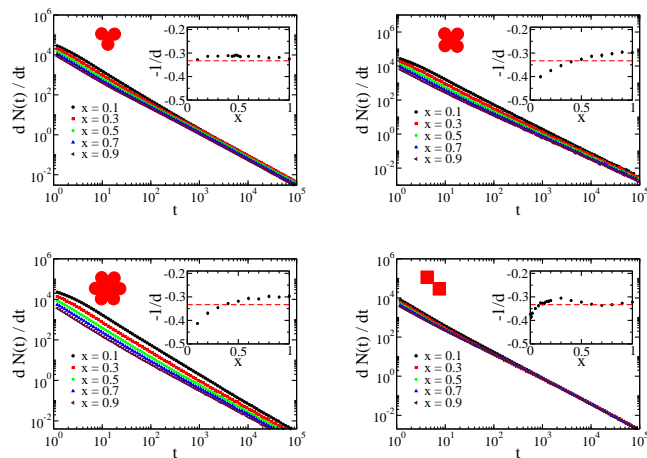


Figure 3. (Color online) RSA kinetics for trimers, tetramers, hexamers and square dimers. Main panels show number of added particles in a time unit versus time. Insets show fitted exponent in Eq. 8 dependence on x . Dashed lines correspond to the $d = 3$ characteristic behavior for anisotropic molecules.

Eq. (8) is fulfilled as the data obtained from numerical simulations lays along straight lines in a log-log scale. The parameter d obtained from fitting numerical data to the relation (8) is, as expected for anisotropic particles, around 3. In a limit of small x , for tetramers and hexamers the drop of d down to 2 is observed, which is expected, as the particle shape arises from disk-like geometry and the simulations have not yet reached the true asymptotic behavior. In other words, the apparent change of d from

3 to 2 as x decreases represents crossover behavior between the two exponents. For trimers this drop occurs for very small x , which resembles its behavior for dimers [21]. In the case of square dimers very slight decrease is observed, because even for $x = 0$ the particle is still anisotropic. This is in agreement with previous observations [26, 27].

B. Saturated random packing fractions

Knowing parameter d and substituting $y = t^{-1/d}$, Eq. (8) can be rewritten in a form: $N(y) = N_{\max} + A'y$. Thus, points $(N(y), y)$ measured during an RSA simulation lie along a straight line which crosses the axis $y = 0$ at N_{\max} . It solves the problem of finite time simulations. Another problem originates in the finite size of a system, which is especially important as periodic boundary conditions are not used here. It is expected that in general the number of particles in a packing are a quadratic function of the surface size: $N(S_C) = aS_C + b\sqrt{S_C} + c$. Thus for an infinite system ($S_C \rightarrow \infty$), a packing density $N(S_C)/S_C = a$. Therefore, to get a packing density in a limit infinitely large systems, several different sized systems should be analyzed to get the a coefficient in the above relation. In this study S_C varies from $2.5 \cdot 10^5$ up to 10^6 . Packing fractions obtained in this way are presented in Fig. 4. For all shapes the maximal packing fraction is reached for $x \in [0, 1]$. This confirms reasoning presented in [17] that anisotropy prefers parallel alignment of particles for large t , which causes increase of packing fraction, but, on the other hand, at the beginning of RSA the anisotropic particle blocks significantly more space than its surface area, which lowers the packing fraction. Thus, the optimum is reached for a small anisotropy. Fitting a quadratic function to the data near the maximum allows us to estimate an optimal anisotropy, which in our case is determined by parameter x , and the value of the highest possible packing fraction. For convenience these data are collected together in the Table I.

shape	x	θ_{\max}
dimer [21]	0.5098	0.5793
trimer	0.4804	0.5705
tetramer	0.3384	0.5541
hexamer	0.2103	0.5505
square dimer	0.1452	0.5364

Table I. Maximal possible saturated packing fractions and corresponding values of parameter x for which they are reached. The statistical error of θ_{\max} does not exceed 0.0001.

IV. DISCUSSION

For all shapes we studied, the maximal possible packing fraction is smaller than for generalized dimers [21].

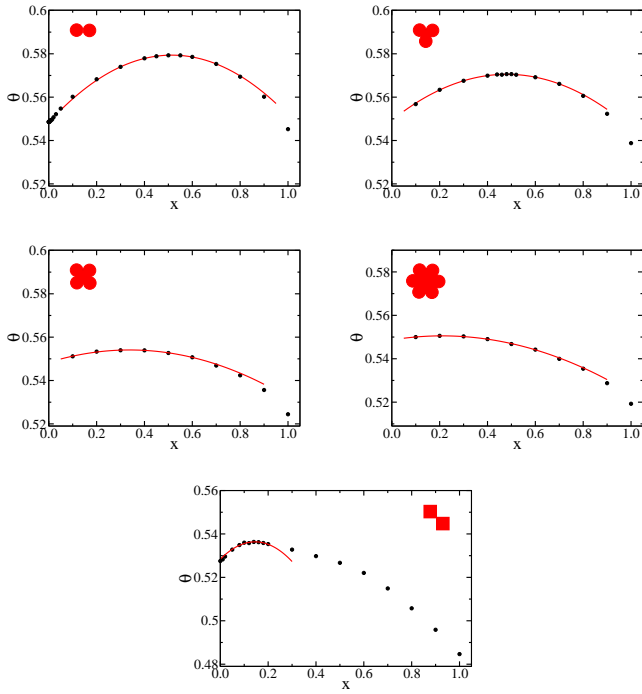


Figure 4. (Color online) Saturated packing fraction dependence on parameter x for trimers, tetramers, hexamers and square dimers. Dots represents data from numerical simulations. Solid red lines are quadratic fits near maxima of θ_{\max} . Data for dimers were taken from [21]. The fits are: $\theta_2 = 0.5483 + 0.12089x - 0.11751x^2$, $\theta_3 = 0.54933 + 0.088299x - 0.091899x^2$, $\theta_4 = 0.54835 + 0.033967x - 0.050194x^2$, $\theta_6 = 0.54867 + 0.017815x - 0.042357x^2$, $\theta_{2s} = 0.52839 + 0.10979x - 0.37802x^2$.

The more complex shape type, the lower the value of the maximum packing fraction. The lowest values are obtain for square dimer. In this last case the θ_{\max} is smaller than for rectangles (0.55) [15, 17] as well as for disks (0.5470) [14]. In all cases it is smaller than value for ellipsoids or spherocylinders (0.583) reported in [15]. However, these dimers, trimers tetramers and hexamers do not have the best possible shape to reach highest random packing fraction. As illustrated in Fig. 5 the small

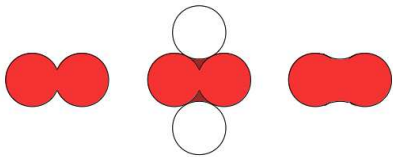


Figure 5. (Color online) The transition from generalized dimer to a shape with larger surface area and the same blocking area.

purple areas in both sides of a dimer cannot be occupied by any other particle. It means that this surface is blocked but it is not counted in the packing fraction. There is a direct projection between packing composed

of dimers and rightmost particles in Fig. 5. Therefore saturated random packing fraction for this shape will be slightly higher than for dimers. Similar reasoning can be performed for trimers, tetramers and hexamers. Note that this reasoning is valid also for $x > 1$, however, too large a value of x can destroy the mentioned projection between two types of shapes. For example for dimer the projection is valid for $x \leq \sqrt{2}$.

The surface area of one of these additional regions is

$$S_{\text{ad}}(x) = \begin{cases} x(\sqrt{4-x^2} - \sqrt{1-x^2}) - \arcsin x & 0 \leq x < 1 \\ x\sqrt{4-x^2} - \frac{\pi}{2} & 1 \leq x \leq \sqrt{3} \end{cases} \quad (9)$$

Taking this into account and performing the same analysis (see Fig. 6) as in Sec. III B the following values are obtained (see Table II). Note that in case of dimers

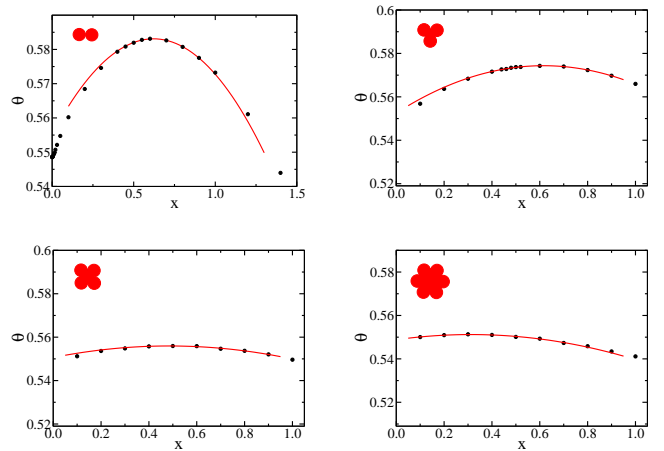


Figure 6. (Color online) Saturated packing fraction dependence on parameter x for dimers, trimers, tetramers and hexamers with additional blocked regions taken into account (“Smoothed” shapes.) Dots represents data from numerical simulations. Solid red lines are quadratic fits near maxima of θ_{\max} . Data for dimers were taken from [21]. The fits are $\theta_2 = 0.55513 + 0.089974x - 0.072349x^2$, $\theta_3 = 0.55253 + 0.070875x - 0.057558x^2$, $\theta_4 = 0.55062 + 0.021978x - 0.022673x^2$, $\theta_6 = 0.54883 + 0.015239x - 0.024414x^2$.

with $x > 1$ the additional surface does not compensate a smaller number of particles in the packing so the packing fraction lowers with growing x . Therefore we focused on $x \leq 1$ in the case of trimers, tetramers and hexamers. The calculated packing fractions are bigger, but the difference is less than 0.005 and becomes smaller with growing number of disks in particle. On the other hand, the value obtained for dimeric particle is now similar to the one for ellipsoids and spherocylinders. As expected, the value of x where the packing reaches a maximum is larger when we include the blocked areas in the particles. For the case of the smoothed out dimer, we are finding a maximum coverage at $x = 0.6347$, or in other words the aspect ratio α (ratio of maximum dimensions in the two directions) is 1.6347. This compares with a maximum for other shapes as given in Table III. Evidently, by making

shape	x	θ_{\max}
dimer	0.6347	0.5833
trimer	0.6146	0.5744
tetramer	0.4969	0.5560
hexamer	0.3036	0.5513

Table II. Maximal possible saturated packing fractions and corresponding values of parameter x for which they are reached. Here the additional blocked regions were taken into account (“smoothed” shapes). The statistical error of θ_{\max} does not exceed 0.0001.

the smoothed concave dimer shape, one is able to reach a coverage comparable to the maximum of certain other convex shapes (the ellipse and spherocylinder). This is because in RSA there is a tendency for particles of moderate aspect ratio to adsorb in a “T” configuration, and having an indentation in the sides of the particles allows one of the disk ends of a neighboring particle to fit in nicely, thus increases the overall coverage. The linear shape also allows the dimers to align in a parallel fashion which occurs at later times in the adsorption process.

shape	α	θ_{\max}	Ref.
rectangle	1.618	0.553(1)	[15]
dimer	1.5098	0.5793(1)	[21]
ellipse	2.0	0.583(1)	[15]
spherocylinder	1.75	0.583(1)	[15]
smoothed dimer	1.6347	0.5833(1)	this work

Table III. Comparison of the maximal coverages for various oblong shapes. α is the aspect ratio, equalling $1+x$ for dimers. Numbers in parentheses are errors in the last digit.

V. SUMMARY

Several anisotropic and concave shapes of particles were analyzed in terms of maximal possible random packing fraction. It was found that the highest packing fraction is obtained for particle built of two disks with additional blocking area (see Fig. 5), where the distance between their centers is 2×0.6347 which interestingly is more than 20% larger than in the case without the extended blocking region. The saturated random packing fraction for such a shape is 0.5833 ± 0.0001 and is at the level of the highest of previously reported values for other particle shapes. Future studies of higher precision can show which of the highest coverage shapes (smoothed dimer, ellipse, or spherocylinder or other oblong object) is the absolute best.

VI. ACKNOWLEDGMENTS

G. Pająk acknowledges support of Cracovian Consortium ‘„Materia-Energia-Przyszłość” im. Mariana Smoluchowskiego’ within the KNOW grant.

-
- [1] P. J. Flory, *J. Am. Chem. Soc.* **61** 1518 (1939)
[2] A. Rényi, *Publ. Math. Inst. Hung. Acad. Sci.* **3** 109 (1958)
[3] J. Feder, *J. Theor. Biol.* **87** 237 (1980)
[4] J. W. Evans, *Rev. Mod. Phys.* **65** 1281 (1993)
[5] Z. Adamczyk, *Curr. Opin. Colloid Interface Sci.* **17** 173 (2012)
[6] A. Dąbrowski, *Adv. Colloid Interface Sci.* **93** 135 (2001)
[7] S. Torquato, F. H. Stillinger, *Rev. Mod. Phys.* **82** 2633 (2010)
[8] E. I. Corwin, M. Clusel, A. O. N. Siemens, J. Brujic, *Soft Mat.* **6** 2949 (2010)
[9] A. V. Kyrilyuk, M. A. van de Haar, L. Rossi, A. Wouterse, A. P. Philipse, *Soft Mat.* **7** 1671 (2011)
[10] C. Zong, *arXiv:1410.1102 [math.MG]* (2014)
[11] M. B. Hastings, *Phys. Rev. E* **72** 015102(R) (2005)
[12] E. G. Coffman Jr, L. Flatto, P. Jelenkovich, B. Poonen, *Algorithmica* **22** 448 (1998)
[13] M. Cieśla, J. Barbasz, *J. Chem. Phys.* **138** 214704 (2013)
[14] G. Zhang, S. Torquato, *Phys. Rev. E* **88** 053312 (2013)
[15] P. Viot, G. Tarjus, S. Ricci, J. Talbot, *J. Chem. Phys.* **97** 5212 (1992)
[16] J. D. Sherwood, *J. Phys. A: Math. Gen.* **23** 2827 (1990)
[17] R. D. Vigil, R. M. Ziff, *J. Chem. Phys.* **91** 2599 (1989)
[18] R. D. Vigil, R. M. Ziff, *J. Chem. Phys.* **93** 8270 (1990)
[19] M. Cieśla, *Phys. Rev. E*, **87** 052401 (2013)
[20] P. B. Shelke, A.V. Limaye, *Surf. Sci.* **637-638** 1 (2015)
[21] M. Cieśla *Phys. Rev. E* **89** 042404 (2014)
[22] M. Cieśla, J. Barbasz *Phys. Rev. E* **89** 022401 (2014)
[23] Y. Pomeau *J. Phys. A: Math. Gen.* **13** L193 (1980)
[24] R. H. Swendsen *Phys. Rev. A* **24** 504 (1981)
[25] E. L. Hinrichsen, J. Feder, T. Jøssang *J. Stat. Phys.* **44** 793 (1986)
[26] P. Viot, G. Tarjus, *Europhys. Lett.* **13** 295 (1990)
[27] M. Cieśla, J. Barbasz *Phys. Rev. E* **90** 022402 (2014)